

論文

균열이 있는 기능경사 압전 세라믹의 충격 특성에 관한 연구

신정우^{*,}, 김태욱^{**}, 김성찬^{**}

Transient Response of Functionally Graded Piezoelectric Ceramic with Crack

Jeong Woo Shin^{*,}, Tae-Uk Kim^{**}, Sung Chan Kim^{**}

ABSTRACT

Using the theory of linear piezoelectricity, the dynamic response of a central crack in a functionally graded piezoelectric ceramic under anti-plane shear impact is analyzed. We assume that the properties of the functionally graded piezoelectric material vary continuously along the thickness. By using the Laplace and Fourier transform, the problem is reduced to two pairs of dual integral equations and then into Fredholm integral equations of the second kind. Numerical values on the dynamic stress intensity factors are presented to show the dependence of the gradient of material properties and electric loading.

초 록

선형 압전 이론(theory of linear piezoelectricity)을 이용하여 면의진단 충격(anti-plane shear impact)을 받는 기능경사 압전 세라믹(functionally graded piezoelectric ceramic)의 중앙에 존재하는 균열(central crack)의 동적 응답에 대해 연구한다. 기능경사 압전재료의 물성치(material property)는 두께방향을 따라 연속적으로 변한다고 가정한다. 라플라스 변환(Laplace transform)과 푸리에 변환(Fourier transform)을 사용하여 두 쌍의 복합적분 방정식을 구성하며, 이를 제2종 Fredholm 적분 방정식(Fredholm integral equations of the second kind)으로 표현한다. 재료 물성치의 변화도(gradient of material properties)와 전기하중(electric loading)의 영향을 보기 위해 동응력세기계수(dynamic stress intensity factor)에 대한 수치 결과를 제시하였다.

Key Words : 압전세라믹(piezoelectric ceramic), 균열(crack), 기능경사재료(functionally graded material), 동응력세기계수(dynamic stress intensity factor)

1. Introduction

Recently, the dynamic response and the failure modes of piezoelectric materials have great attention from many researchers. Shindo and Ozawa[1] first investigated the steady response of a cracked piezoelectric material under the action of incident plane harmonic waves. A finite crack in an infinite piezoelectric material under anti-plane dynamic electro-mechanical impact was investigated by Chen and Yu[2] with well-established integral transform methodology.

Axisymmetric vibration of piezo-composite hollow cylinder was studied by Paul and Nelson[3]. The dynamic representation formulas and fundamental solutions for piezoelectricity was proposed by Khutoryansky and Sosa[4]. The dynamic response of a cracked dielectric medium under the action of harmonic waves in a uniform electric field was studied by Shindo *et al.*[5]. Li and Mataga[6,7] studied the semi-infinite propagating crack in a piezoelectric material with electrode boundary condition and vacuum boundary condition on the crack surface, respectively. In the work, the transient

*+ 한국항공우주연구원, 연구원, 교신저자(E-mail:jeongdal@kari.re.kr)

** 한국항공우주연구원, 선임연구원

dynamic electro-mechanical loads were taken into consideration. Chen[8] obtained the solution of the infinite piezoelectric strip parallel to the crack under anti-plane shear impact loading using integral transform method. However, most researches examined homogeneous models and few fracture mechanics research of functionally graded piezoelectric material are presented. Shin and Kim[9] studied the crack problem for functionally graded piezoelectric ceramic strip using integral transform techniques. They considered the static electro-mechanical loading with permeable crack boundary condition.

Applying the electric boundary condition for the crack, many researchers have adopted two different boundary conditions.

Parton[10], Zhang and Hak[11] and Hao and Shen[12] proposed a permeable crack boundary condition which assumes the continuity of electric displacement across the crack faces. On the contrary, Deeg[13], Sosa[14] and Pak[15] adopted an impermeable crack boundary condition, i.e., the vanishing of normal electric displacement on the crack faces. Also, Kumar and Singh[16] showed the validation of impermeable condition using FEM analysis. But these two boundary conditions have not been verified yet, so each researcher presented different results.

Recently, Xu and Rajapakse[17] found that the exact electric boundary conditions accounting for the medium inside the crack gaps would be reduced to the impermeable crack model when the poling direction is perpendicular to the applied electric field, so impermeable boundary condition is more suitable in this paper.

In this paper, we study the problem of a finite central crack in a functionally graded piezoelectric ceramic medium under anti-plane shear impact loading based on the dynamic theory of linear electroelasticity. We assume that the properties of the functionally graded piezoelectric material vary continuously along the thickness. The impermeable crack boundary condition is adopted. By using the Laplace and Fourier transform, the problem is reduced to two pairs of dual integral equations and then into Fredholm integral equations of the second kind. Numerical results for the stress intensity factors are shown graphically.

2. Problem statement and method of solution

Consider a functionally graded piezoelectric medium in the form of an infinite body containing a finite central crack

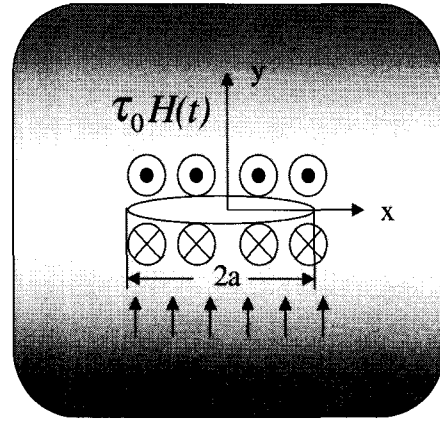


Fig. 1 A functionally graded piezoelectric ceramic medium with crack : definition of geometry and loading.

subjected to mechanical and electric Heaviside step pulse loadings as shown in Fig. 1. A set of cartesian coordinates(x, y, z) is attached to the center of the crack. The piezoelectric ceramic body poled with z-axis and is thick enough in the z-direction to allow a state of anti-plane shear. The crack is situated along the central line $(-a \leq x \leq a, y=0)$. Because of the symmetry in geometry and loading, it is sufficient to consider only the right-hand half body.

We assume that the properties of the functionally graded piezoelectric ceramic strip vary continuously along the thickness and are simplified as follows(Erdogan[18]),

$$c_{44} = c_{44}^0 e^{\beta y} \quad (1)$$

$$d_{11} = d_{11}^0 e^{\beta y} \quad (2)$$

$$e_{15} = e_{15}^0 e^{\beta y} \quad (3)$$

where c_{44} is the elastic modulus measured in a constant electric field, d_{11} is the dielectric permittivity measured at a constant strain and e_{15} is the piezoelectric constant. c_{44}^0 , d_{11}^0 and e_{15}^0 are material properties at $y=0$, and β is the non-homogeneous material constant.

The piezoelectric boundary value problem is simplified considerably if we consider only the out-of-plane displacement and the in-plane electric fields such that

$$u_x = u_y = 0, \quad u_z = w(x, y, t), \quad (4)$$

$$E_x = E_x(x, y, t), \quad E_y = E_y(x, y, t), \quad (5)$$

$$E_z = 0$$

where u_k and E_k ($k = x, y, z$) are displacements and electric fields, respectively.

In this case, the constitutive relations become

$$\sigma_{zj}(x, y, t) = c_{44}w_{,j} + e_{15}\phi_{,j}, \quad (6)$$

$$D_j(x, y, t) = e_{15}w_{,j} - d_{11}\phi_{,j}. \quad (7)$$

where σ_{zj} and D_j ($j = x, y$) are the stress components and electric displacements, respectively.

The dynamic anti-plane governing equations for functionally graded piezoelectric materials are simplified as follows,

$$c_{44}\nabla^2 w + e_{15}\nabla^2 \phi + \beta(c_{44}\frac{\partial w}{\partial y} + e_{15}\frac{\partial \phi}{\partial y}) = \rho\frac{\partial^2 w}{\partial t^2}, \quad (8)$$

$$e_{15}\nabla^2 w - d_{11}\nabla^2 \phi + \beta(e_{15}\frac{\partial w}{\partial y} - d_{11}\frac{\partial \phi}{\partial y}) = 0, \quad (9)$$

where $\nabla^2 = \partial^2/\partial x^2 + \partial^2/\partial y^2$ is the two dimensional Laplace operator and ρ is a material density. We also assume the material density is as follows,

$$\rho = \rho^0 e^{\beta y}. \quad (10)$$

From Eqs. (8) and (9), we can obtain the equation of wave motion in a form,

$$\nabla^2 w + \beta\frac{\partial w}{\partial y} = \frac{1}{c_2^2}\frac{\partial^2 w}{\partial t^2}, \quad (11)$$

where $c_2 = \sqrt{\mu^0/\rho^0}$ and $\mu^0 = c_{44}^0 + e_{15}^0{}^2/d_{11}^0$. The Laplace transform of Eq. (11) is in the form,

$$\nabla^2 w^* + \beta\frac{\partial w^*}{\partial y} = \frac{p^2}{c_2^2} w^*, \quad (12)$$

where

$$w^*(x, y, p) = \int_0^\infty w(x, y, t) e^{-pt} dt, \quad (13)$$

$$w(x, y, t) = \frac{1}{2\pi i} \int_{c-i\infty}^{c+i\infty} w^*(x, y, p) e^{pt} dp. \quad (14)$$

The superscript * stands for the Laplace transform domain.

A Fourier transform is applied to the Laplace transform of Eqs. (9) and (12), and the results are

$$w^*(x, y, p) = \frac{2}{\pi} \int_0^\infty A_1(s, p) e^{-sy} \cos(sx) ds, \quad (15)$$

$$\phi^*(x, y, p) = \frac{2}{\pi} \int_0^\infty [\frac{e_{15}^0}{d_{11}^0} A_1(s, p) e^{-sy} + A_2(s, p) e^{-ry}] \cos(sx) ds, \quad (16)$$

where

$$q = \delta + \frac{\beta}{2}, \quad r = \lambda + \frac{\beta}{2}, \quad (17)$$

$$\delta = \sqrt{\gamma^2 + \frac{\beta^2}{4}}, \quad \lambda = \sqrt{s^2 + \frac{\beta^2}{4}}, \quad (18)$$

$$\gamma = \sqrt{s^2 + \frac{p^2}{c_2^2}}. \quad (19)$$

$A_1(s, p)$ and $A_2(s, p)$ are the unknowns to be solved.

The boundary conditions in the Laplace transform domain can be written as

$$\sigma_{yz}^*(x, 0, p) = -\tau_0/p, \quad (0 \leq x < a), \quad (20)$$

$$w^*(x, 0, p) = 0, \quad (a \leq x < \infty),$$

$$D_y^*(x, 0, p) = -D_0/p, \quad (0 \leq x < a), \quad (21)$$

$$\phi^*(x, 0, p) = 0, \quad (a \leq x < \infty).$$

From the two mixed boundary conditions Eqs. (20) and (21), we can obtain the following two simultaneous dual integral equations,

$$\begin{aligned} \frac{2}{\pi} \int_0^\infty q A_1(s, p) \cos(sx) ds = \\ \frac{1}{p} \frac{d_{11}^0 \tau_0 + e_{15}^0 D_0}{c_{44}^0 d_{11}^0 + e_{15}^0{}^2}, \quad (0 \leq x < a), \\ \int_0^\infty A_1(s, p) \cos(sx) ds = 0, \quad (a \leq x < \infty), \end{aligned} \quad (22)$$

$$\frac{2}{\pi} \int_0^{\infty} r A_2(s, p) \cos(sx) ds = -\frac{1}{p} \frac{D_0}{d_{11}^0}, \quad (0 \leq x < a), \quad (23)$$

$$\int_0^{\infty} A_2(s, p) \cos(sx) ds = 0, \quad (a \leq x < \infty).$$

Eqs. (22) and (23) may be solved by using new functions $\Phi_1^*(\xi, p)$ and $\Phi_2^*(\xi, p)$ defined by

$$A_1(s, p) = \int_0^a \xi \Phi_1^*(\xi, p) J_0(s\xi) d\xi, \quad (24)$$

$$A_2(s, p) = \int_0^a \xi \Phi_2^*(\xi, p) J_0(s\xi) d\xi, \quad (25)$$

where $J_0()$ is the zero-order Bessel function of the first kind.

Inserting Eq. (24) into Eq. (22), we can find that the auxiliary function $\Phi_1^*(\xi, p)$ is given by a Fredholm integral equation of the second kind in the form,

$$\begin{aligned} \Phi_1^*(\xi, p) + \int_0^a K(\xi, \eta, p) \Phi_1^*(\eta, p) d\eta \\ = \frac{\pi}{2} \frac{1}{p} \frac{d_{11}^0 \tau_0 + e_{15}^0 D_0}{c_{44}^0 d_{11}^0 + e_{15}^0{}^2}, \end{aligned} \quad (26)$$

where

$$K(\xi, \eta, p) = \eta \int_0^{\infty} (q-s) J_0(s\eta) J_0(s\xi) ds. \quad (27)$$

For the sake of convenience, we define the following non-dimensional quantities,

$$\eta = aH, \quad \xi = a\bar{\xi}, \quad (28)$$

$$s = \frac{S}{a}, \quad \beta = \frac{B}{a}, \quad q = \frac{Q}{a}, \quad (29)$$

$$\Phi_1^*(\xi, p) = \frac{\pi}{2} \frac{1}{p} \frac{d_{11}^0 \tau_0 + e_{15}^0 D_0}{c_{44}^0 d_{11}^0 + e_{15}^0{}^2} \frac{\Psi_1^*(\bar{\xi}, p)}{\sqrt{\bar{\xi}}}, \quad (30)$$

$$\Phi_2^*(\eta, p) = \frac{\pi}{2} \frac{1}{p} \frac{d_{11}^0 \tau_0 + e_{15}^0 D_0}{c_{44}^0 d_{11}^0 + e_{15}^0{}^2} \frac{\Psi_2^*(H, p)}{\sqrt{H}}. \quad (31)$$

Putting Eqs. (28)~(31) into Eqs. (26) and (27), the following Fredholm integral equation of the second kind is obtained,

$$\Psi_1^*(\bar{\xi}, p) + \int_0^1 L_1(\bar{\xi}, H, p) \Psi_1^*(H, p) dH = \sqrt{\bar{\xi}}, \quad (32)$$

where

$$\begin{aligned} L_1(\bar{\xi}, H, p) = \sqrt{\bar{\xi}H} \int_0^{\infty} S(Q/S-1) \\ \times J_0(SH) J_0(S\bar{\xi}) dS, \end{aligned} \quad (33)$$

Applying the similar way to Eqs. (23) and (25), we can also obtain following Fredholm integral equation of the second kind,

$$\Psi_2^*(\bar{\xi}, p) + \int_0^1 L_2(\bar{\xi}, H, p) \Psi_2^*(H, p) dH = \sqrt{\bar{\xi}}, \quad (34)$$

where

$$\begin{aligned} L_2(\bar{\xi}, H, p) = \sqrt{\bar{\xi}H} \int_0^{\infty} S(R/S-1) \\ \times J_0(SH) J_0(S\bar{\xi}) dS, \end{aligned} \quad (35)$$

$$r = R/a. \quad (36)$$

$$\Phi_2^*(\xi, p) = -\frac{\pi}{2} \frac{1}{p} \frac{D_0}{d_{11}^0} \frac{\Psi_2^*(\bar{\xi}, p)}{\sqrt{\bar{\xi}}}, \quad (37)$$

$$\Phi_2^*(\eta, p) = -\frac{\pi}{2} \frac{1}{p} \frac{D_0}{d_{11}^0} \frac{\Psi_2^*(H, p)}{\sqrt{H}}. \quad (38)$$

3. Dynamic Intensity Factors

The mode III dynamic stress intensity factor($K_{III}^{\sigma}(p)$) and dynamic electric displacement intensity factor($K_{III}^D(p)$) in the Laplace transform domain are determined by the following formula,

$$\begin{aligned} K_{III}^{\sigma}(p) = \lim_{x \rightarrow a} \sqrt{2\pi(x-a)} \\ \times \{ \sigma_{yz}^*(x, 0, p) - i \sigma_{xz}^*(x, 0, p) \} \\ = \frac{1}{p} \sqrt{\pi a} \left[(\tau_0 + \frac{e_{15}^0}{d_{11}^0} D_0) \Psi_1^*(1, p) - \frac{e_{15}^0}{d_{11}^0} D_0 \Psi_2^*(1, p) \right], \end{aligned} \quad (39)$$

$$\begin{aligned} K_{III}^D(p) = \lim_{x \rightarrow a} \sqrt{2\pi(x-a)} \\ \times \{ D_y^*(x, 0, p) - i D_x^*(x, 0, p) \} \end{aligned} \quad (40)$$

$$= \frac{1}{p} \sqrt{\pi a} D_0 \Psi_2^*(1).$$

From the inverse Laplace transform of Eqs. (39) and (40), we can obtain the dynamic intensity factors in the physical space in the form,

$$K_{III}^r(t) = \sqrt{\pi a} \left[\left(\tau_0 + \frac{e_{15}^0}{d_{11}^0} D_0 \right) M(t) - \frac{e_{15}^0}{d_{11}^0} D_0 \Psi_2^*(1) H(t) \right], \quad (41)$$

$$K_{III}^D(t) = \sqrt{\pi a} D_0 \Psi_2^*(1) H(t), \quad (42)$$

where

$$M(t) = \frac{1}{2\pi i} \int_{c-i\infty}^{c+i\infty} \frac{\Psi_1^*(1, p)}{p} e^{pt} dp. \quad (43)$$

and the functions $\Psi_1^*(1, p)$ and $\Psi_2^*(1)$ is calculated from Eqs. (32) and (34).

Since $\Psi_2^*(1) = 1$ and $Q = \Gamma(\Gamma = \gamma \cdot a)$ in Eqs. (32)~(35) and (43) as $\beta = 0$, dynamic intensity factors for an infinite piezoelectric ceramic can be obtained from Eqs. (41) and (42) in the form,

$$K_{III}^r(t) = \sqrt{\pi a} \left[\left(\tau_0 + \frac{e_{15}^0}{d_{11}^0} D_0 \right) M(t) - \frac{e_{15}^0}{d_{11}^0} D_0 H(t) \right], \quad (44)$$

$$K_{III}^D(t) = \sqrt{\pi a} D_0 H(t). \quad (45)$$

This solution agrees with that of Chen and Yu[2].

4. Numerical results and discussions

To examine the effect of electro-mechanical interactions on the dynamic stress intensity factors, Eqs. (32) and (34) are computed numerically by Gaussian quadrature formulas. The inverse Laplace transformations of the intensity factors are carried out by the numerical method described by Miller and Guy[19]. We assume that piezoelectric material properties at $y = 0$ are same as PZT-5H which are listed in Table 1.

Table 1 Material properties of piezoelectric ceramic at $y=0$

Properties	Symbol	Unit	
Elastic stiffness	c_{44}^0	$\times 10^{10} \text{ N/m}^2$	2.3
Piezoelectric constant	e_{15}^0	C/m^2	17.0
Permittivity	d_{11}^0	$\times 10^{-10} \text{ F/m}$	150.4

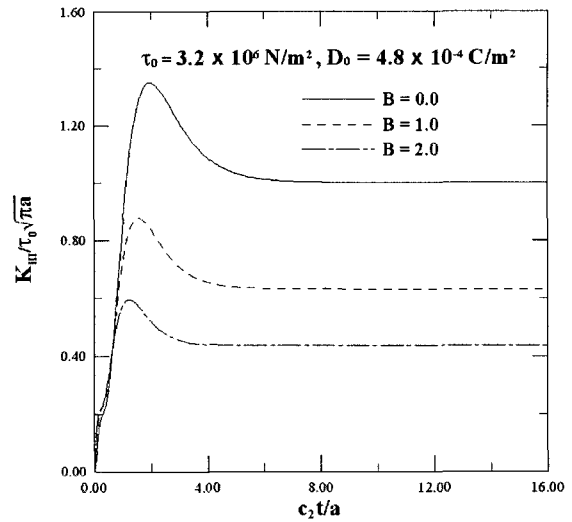


Fig. 2 Stress intensity factor $K_{III}/\tau_0\sqrt{\pi a}$ versus c_2t/a with various values of B .

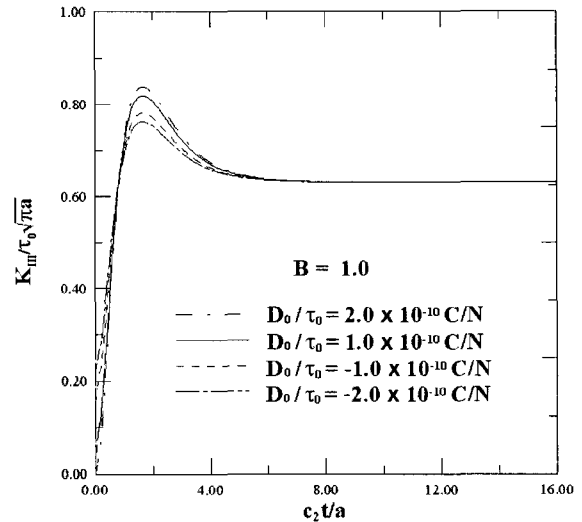


Fig. 3 Stress intensity factor $K_{III}/\tau_0\sqrt{\pi a}$ versus c_2t/a with various values of D_0/τ_0 at $B=1.0$.

Fig. 2 displays the variations of the normalized dynamic stress intensity factor $K_{III}/\tau_0\sqrt{\pi a}$ against normalized time c_2t/a with various B values at $\tau_0 = 3.2 \times 10^6 \text{ N/m}^2$ and $D_0 = 4.8 \times 10^4 \text{ C/m}^2$.

The normalized dynamic stress intensity factor rises rapidly with time, reaching a peak, then decrease in magnitude to reach static values. The larger value B , the faster time arriving at peak values. Peak values decrease as B value

increases. We can show that increasing the FGM(functionally gradient material) gradient is helpful to the reduction of the dynamic stress intensity factor.

Fig. 3 shows the variations of the normalized dynamic stress intensity factor $K_{III}/\tau_0\sqrt{\pi a}$ against normalized time $c_2 t/a$ with various D_0/τ_0 values at $B=1.0$. Peak values increase as the positive D_0/τ_0 value increases, but peak values decrease when the negative D_0/τ_0 value increases. It shows that the negative D_0/τ_0 values helps the reduction of the dynamic stress intensity factor.

5. Conclusions

The electroelastic problem of a central crack in a functionally graded piezoelectric ceramic medium under anti-plane impact shear was analyzed by the integral transform approach. The properties and mass density of the functionally graded piezoelectric material vary continuously along the thickness. The impermeable crack boundary condition is adopted. The traditional concept of linear elastic fracture mechanics is extended to include the piezoelectric effects and the results are expressed in terms of the dynamic stress intensity factor and dynamic electric displacement intensity factor. Dynamic stress intensity factor is dependent on both stress and electric impact loads, but dynamic electric displacement intensity factor is only related to the electric impact loading. And the computed results show that dynamic stress intensity factor can be greatly reduced by increasing the gradient of the material properties and negative electric displacement.

References

- 1) Y. Shindo and E. Ozawa, "Dynamic Analysis of a Piezoelectric Material. In: Mechanical Modeling of New Electromagnetic Materials," (ed. R. K. T. Hsieh), Elsevier Science Publishers B. V., 1990, pp. 297-304.
- 2) Z. T. Chen and S. W. Yu, "Anti-plane Dynamic Fracture Mechanics in Piezoelectric Materials," *International Journal of fracture*, Vol. 85, 1997, pp. L3-L12.
- 3) H S. Paul and V. K. Nelson, "Axisymmetric Vibration of Piezo-composite Hollow Circular Cylinder," *Acta Mechanica* Vol. 116, 1996, pp. 213-222.
- 4) N. M. Khutoryansky and H. Sosa, "Dynamic Representation Formulas and Fundamental Solutions for Piezoelectricity," *International Journal of Solids and Structures*, Vol. 32, 1995, pp. 3307-3325.
- 5) Y. Shindo, H. Katsura, and W. Yan, "Dynamic Stress Intensity Factor of a Cracked Dielectric Medium in a Uniform Electric Field," *Acta Mechanica*, Vol. 117, 1996, pp. 1-10.
- 6) S. Li and PA. Mataga, "Dynamic crack propagation in piezoelectric materials - part I. electrode solution," *Journal of the Mechanics and Physics of Solids*, Vol. 44, No. 11, 1996, pp. 1799-1830.
- 7) S. Li and PA. Mataga, "Dynamic crack propagation in piezoelectric materials - part II. vacuum solution," *Journal of the Mechanics and Physics of Solids*, Vol. 44, No. 11, 1996, pp. 1831-1866.
- 8) Z. T. Chen, "Crack tip field of an infinite piezoelectric strip under anti-plane impact," *Mechanics Research Communications*, Vol. 25, 1998, pp. 313-319.
- 9) J. W. Shin and S. C. Kim, "The Crack Problem for Functionally Graded Piezoelectric Ceramic Strip," *Journal of The Korean Society for Composite Materials*, Vol. 15, No. 4, pp. 37-42.
- 10) V. Z. Parton, "Fracture Mechanics of Piezoelectric Materials," *Acta Astronautica*, Vol. 3, 1976, pp. 671-683.
- 11) T. Y. Zhang, and J. E. Hack, "Mode III Cracks in Piezoelectric Materials," *Journal of Applied Physics*, Vol. 71, 1992, pp. 5865-5870.
- 12) T. H. Hao, and Z. T. Shen, "A New Electric Boundary Condition of Electric Fracture Mechanics and Its Applications," *Engineering Fracture Mechanics*, Vol. 47, 1994, pp. 793-802.
- 13) W. F. Deeg, "The Analysis of Dislocation, Crack, and Inclusion Problems in Piezoelectric Solids," Ph. D. Thesis, Stanford University, Stanford, CA., 1980.
- 14) H. Sosa, "On the Fracture Mechanics of Piezoelectric Solids," *International Journal of Solids and Structures*, Vol. 29, 1992, pp. 2613-2622.
- 15) Y. E. Pak, "Linear Electroelastic Fracture Mechanics of Piezoelectric Materials," *International Journal of Fracture*, Vol. 54, 1992, pp. 79-100.
- 16) S. Kumar, and R. N. Singh, "Influence of Applied Electric Field and Mechanical Boundary Condition on the Stress Distribution at the Crack Tip in Piezoelectric Materials," *Materials Science and Engineering*, Vol. A231, 1997, pp. 1-9.

- 17) X.-L. Xu, and R.K.N.D. Rajapakse, "On a plane crack in piezoelectric solids," *International Journal of Solids and Structures*, Vol. 38, 2001, pp. 7643-7658.
- 18) F. Erdogan, "The crack problem for bonded nonhomogeneous materials under antiplane shear loading," ASME, *Journal of Applied Mechanics*, Vol. 52, 1985, pp. 823-828.
- 19) M. K. Miller and W. T. Guy, "Numerical Inversion of the Laplace Transform by Use of Jacobi Polynomials," *SIAM Journal on Numerical Analysis*, Vol. 3, 1966, pp. 624-635.